

Design of augmented reality display based on polarization grating

Renjie Xia(夏人杰), Changshun Wang(王长顺), Yujia Pan(潘雨佳), Tianyu Chen(陈天宇), Ziyao Lyu(吕子瑶), Lili Sun(孙丽丽)

Citation: Chin. Phys. B . 2019, 28(7): 074201. **doi:** 10.1088/1674-1056/28/7/074201
Journal homepage: http://cpb.iphy.ac.cn; http://iopscience.iop.org/cpb

What follows is a list of articles you may be interested in

Macadam's theory in RGB laser display

Guan Wang(王贯), Yuhua Yang(杨雨桦), Tianhao Dong(董天浩), Chun Gu(顾春), Lixin Xu(许立新), Zhongcan Ouyang(欧阳钟灿), Zuyan Xu(许祖彦)

Chin. Phys. B . 2019, 28(6): 064209. **doi:** 10.1088/1674-1056/28/6/064209

Holographic storage of three-dimensional image and data using photopolymer and polymer dispersed liquid crystal films

Hong-Yue Gao(高洪跃), Pan Liu(刘攀), Chao Zeng(曾超), Qiu-Xiang Yao(姚秋香), Zhiqiang Zheng(郑志强), Jicheng Liu(刘吉成), Huadong Zheng(郑华东), Ying-Jie Yu(于瀛洁), Zhen-Xiang Zeng(曾震湘), Tao Sun(孙涛)

Chin. Phys. B . 2016, 25(9): 094205. **doi:** 10.1088/1674-1056/25/9/094205

Electrically tunable holographic polymer templated blue phase liquid crystal grating

He Zheng-Hong, Chen Chao-Ping, Zhu Ji-Liang, Yuan Ya-Chao, Li Yan, Hu Wei, Li Xiao, Li Hong-Jing, Lu Jian-Gang, Su Yi-Kai

Chin. Phys. B . 2015, 24(6): 064203. **doi:** 10.1088/1674-1056/24/6/064203

OH^- absorption and nonvolatile holographic storage properties in Mg:Ru:Fe:$LiNbO_3$ crystal as a function of Mg concentration

Xu Chao, Zhang Chun-Lei, Dai Li, Leng Xue-Song, Xu Lei, Xu Yu-Heng

Chin. Phys. B . 2013, 22(5): 054203. **doi:** 10.1088/1674-1056/22/5/054203

Design of an augmented reality display based on polarization grating*

Renjie Xia(夏人杰), Changshun Wang(王长顺)†, Yujia Pan(潘雨佳), Tianyu Chen(陈天宇), Ziyao Lyu(吕子瑶), and Lili Sun(孙丽丽)

State Key Laboratory of Advanced Optical Communication Systems and Networks, School of Physics and Astronomy, Shanghai Jiao Tong University, Shanghai 200240, *China*

(Received 27 January 2019; revised manuscript received 3 April 2019; published online 31 May 2019)

A new optical system for an augmented reality (AR) display is proposed in this paper. The optical system mainly includes a ray deflector, coupling input grating, optical waveguide, and coupling output grating. Both the ray deflector and the coupling input grating are designed based on the diffraction characteristics of the polarization grating, and the coupling output grating is the Bragg reflection grating. Compared with other AR schemes, this AR optical system not only reduces the number of projections from two to one, but also improves the efficiency of light coupling into the optical waveguides. The energy loss is reduced by utilizing the single-order diffraction characteristics of the polarization grating in its coupling input structure. The light deflector uses the polarization selectivity of the polarization grating and the characteristics of the rotating light of the twisted nematic liquid crystal layer to realize beam deflection. The working principle of the optical system is experimentally and theoretically demonstrated.

Keywords: augmented reality, polarization grating, azo liquid crystal

PACS: 42.40.Eq, 42.40.Ht, 42.40.My **DOI:** 10.1088/1674-1056/28/7/074201

1. Introduction

Augmented reality (AR) technology, as a current research hot spot, has attracted many researchers' attention.[1–5] It uses a specially designed optical system to project the calculated image to the human eye so that the observer can see the virtual image generated by the computer while observing real things, thus enhancing the human visual experience. By connecting the real world with the virtual world, AR technology has a lot of remarkable application prospects in many fields, such as medical treatment, communication, maintenance, and entertainment.[6,7] At present, this technology generally exists in the form of a wearable helmet or smart glasses.[8,9] Scientists have come up with many hardware solutions and designed various optical systems to bring this technology into practice.[10–15] These include reflection prisms, free-form surfaces, holographic grating waveguides,[16] pointing light sources,[17] optical field technology, and so on.[18,19] For example, a color transparent screen using planar glass combined with a lens array holographic optical element was proposed Liu *et al.*[20] for a two-dimensional image transparent display. An optical see-through head-mounted display with free-form surface elements, with a diagonal field of view of 50°, was proposed by Wang *et al.*[21] Gao *et al.*[22] proposed and developed a true see-through three-dimensional head mount display system based on the wave-front modulation with a holographic grating filter. Kim *et al.*[23] developed a multi-focus three-dimensional display that gives full parallax monocular depth cues, and omni-directional focus was developed with the least parallax images. The key factor of this display system is a slanted array of the light-emitting diode light source. These schemes have many common bottlenecks to overcome, such as a small viewing angle, low brightness of the image in the field of vision, non-zoom of the image, and too short of a standby time. To improve the coupling efficiency, Lee *et al.* developed a compact and lightweight optical system for AR displays with depth information using Pancharatnam–Berry optical elements as a deflector or as a lens.[24] In order to solve the contradiction between low brightness and short standby time caused by the low optical coupling efficiency of the AR optical system, we proposed an AR optical system based on a polarization grating. The system can greatly improve the coupling efficiency of light entering the optical waveguide. At the same time, the number of micro projections can be reduced from two to one by using the time division multiplexing principle, which can significantly reduce the energy consumption in the use of see-through glasses. The research on polarization gratings has a history of 30 or 40 years. Due to the photoisomerization of azo materials, polarization gratings mainly use azo materials as substrates. Many studies about their various physical and chemical properties have been carried out.[25–31] Polarization gratings have been widely used in optical logic calculations, optical switches, and optical information storage.[32–36] These applications are basically attributed to their diffraction characteristics. In this paper, an optical system based on the polarization grating was proposed. The working principle of the optical system was experimentally and theoretically demonstrated. The polarization grating was recorded and its diffraction mode was studied. In order

*Project supported by the National Natural Science Foundation of China (Grant No. 11574211).

†Corresponding author. E-mail: cswang@sjtu.edu.cn

© 2019 Chinese Physical Society and IOP Publishing Ltd

to ensure the feasibility of this optical system in practice, the relationship between the incident angle and the diffraction angle, and that between the incident angle and the diffraction efficiency, were also investigated.

2. Principle of the optical system

The polarization grating is recorded by orthogonal polarization interference, and is generally divided into the orthogonal linear polarization grating and the orthogonal circular polarization grating. The polarization grating used in this paper is an orthogonal circular polarization grating, which records the interference light field of left and right circular polarizations. The grating will have different diffraction modes according to the polarization of the incident light. The schematic diagram of its diffraction principle is shown in Fig. 1.

It can be seen that there are three kinds of diffraction modes according to the polarization state of the incident light. When the incident light is S-linearly or P-linearly polarized, there are diffractions of the -1 order and $+1$ order, as shown in Figs. 1(a) and 1(b). When the incident light is left-handed circularly polarized, there is only the diffraction of the -1 order, as shown in Fig. 1(c). Furthermore, in Fig. 1(d), when the incident light is right-handed circularly polarized, there is only the diffraction of the $+1$ order. If the thickness of the grating film L, its optical anisotropy Δn and the wavelength λ of the incident light meet the half-wave condition $L\Delta n = \lambda/2$, and the diffraction efficiency can reach 100% in theory.

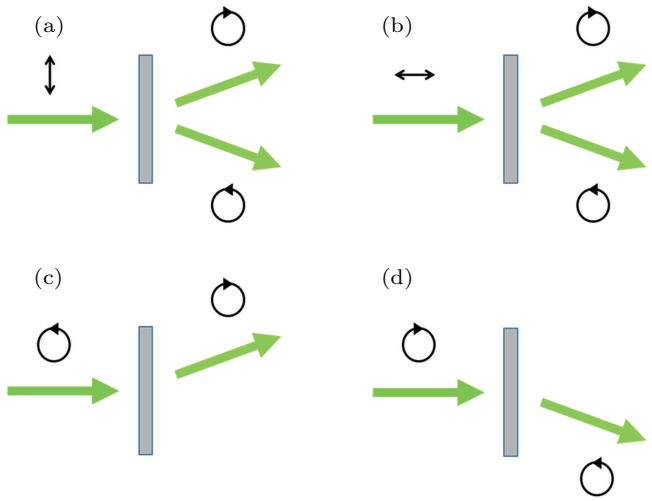


Fig. 1. Diagram of diffraction characteristics of the orthogonal circular polarization grating. The incident light is (a) S-linearly polarized, (b) P-linearly polarized, (c) left-handed circularly polarized, and (d) right-handed circularly polarized.

Based on the diffraction characteristics of polarization gratings and the characteristics of the rotating light of the twisted nematic liquid crystals, a new AR optical system is proposed. The schematic diagram of the optical system structure is shown in Fig. 2.

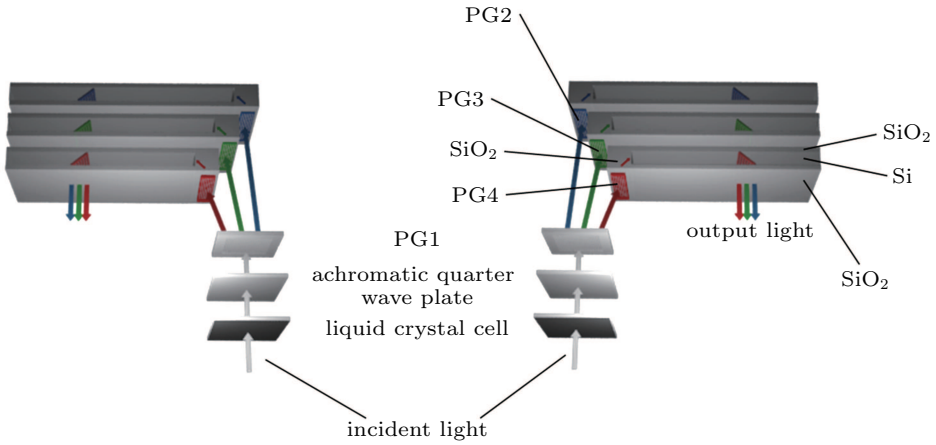


Fig. 2. Schematic diagram of the optical system structure. PG1, PG2, PG3, and PG4 represent four polarization gratings with different grating periods and film thicknesses.

The AR optical system is based on the principle of time division multiplexing, and therefore only one microprojection is needed. We assume that the projected light from the microprojection is S-linearly polarized, and it will first pass through the twisted nematic liquid crystal cell of the system. The upper and lower sides of the liquid crystal cell are covered with transparent electrode layers, which can form a vertical electric field in the liquid crystal cell by adding a voltage. When no voltage is applied to the transparent electrode layers, there is no electric field in the cell. When light passes through the cell, its linear polarization will be rotated by 90°, that is, it changes from S-linear polarization to P-linear polarization. The P-linearly polarized light passes through an achromatic quarter-wave plate and turns into a left-handed circularly polarized light. The left-handed circularly polarized light incident on the polarization grating (PG1) produces the -1 order diffraction. Because the diffraction angle of the polarization grating is related to the wavelength, the white light will be diffracted into three beams of red, green, and blue. Since the beams have different diffraction angles, they incident on the correspond-

ing polarization gratings (PG4, PG3, PG2) of different optical waveguides. Each beam of light enters its own optical waveguide diffracted by the corresponding polarization grating. The three beams of light propagate forward in the optical waveguides by total reflection. Finally, they are emitted from the optical waveguides through the corresponding coupled output gratings, and then projected to the left eye of the person. If voltage is applied to the transparent electrode layer, there is a vertical electric field in the cell, and the long axis of the liquid crystal molecules in the cell will be arranged parallel to the electric field. At this time, the characteristics of the rotating light of the twisted nematic liquid crystals will be lost, and the linear polarization of light will not be changed when light passes through it, that is, the S-linearly polarized light will still be S-linearly polarized after it passes through the liquid crystal cell. Then the S-linearly polarized light passes through the achromatic quarter-wave plate and turns into right-handed circularly polarized light. The right-handed circularly polarized light incident on the polarization grating PG1 produces the $+1$ order diffraction. Similarly, because the diffraction angle of the polarization grating is related to the wavelength, the white light incident on the polarization grating will be divided into three beams of red, green, and blue. Light travels in the same way as described above, and finally enters the right eye.

When the voltage is not applied to the transparent electrode layer, the image of the left view of the object should be loaded into the projector. When the voltage is applied to the transparent electrode layer, the image of the right view of the object should be loaded into the projector. By controlling the voltage switch of the twisted nematic liquid crystals cell, the direction of image output can be controlled to realize three-dimensional display.

3. Experiments and theory

3.1. Polarization grating recording and study

In order to verify the working principle of the optical system, the polarization grating was written. We chose an azo polymer liquid crystal film as the substrate of our grating, and the thickness of the film was about 20 μm. It had good stability and could keep the recorded grating for a long time. A polarization grating actually records the interference light field of the polarized light. In order to facilitate the subsequent grating writing, first, the relationship between the photoinduced birefringence of the azo liquid crystal and the time of the pumping light was investigated, as shown in Fig. 3.

From Fig. 3, we can see that when the pump light is turned on, the photoinduced birefringence of the azo liquid crystal increases rapidly. It reaches the maximum value and remains stable after a few minutes. When the pump light is turned off, the birefringence decreases slightly and tends to stabilize immediately. From the data, it can be seen that the azo liquid crystal polymer has obvious photoinduced birefringence and is suitable for recording gratings. The experimental optical paths of recording the grating and detecting the diffraction light of the grating are shown in Fig. 4.

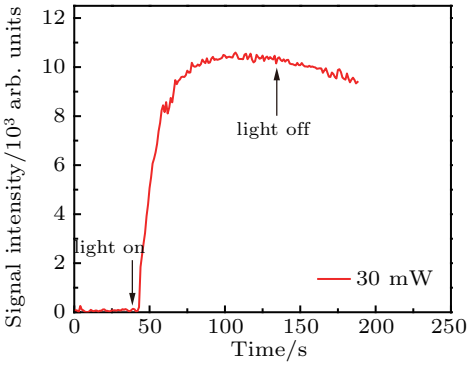


Fig. 3. Photoinduced birefringence curve of azo liquid crystals. The power of the pump light is 30 mW.

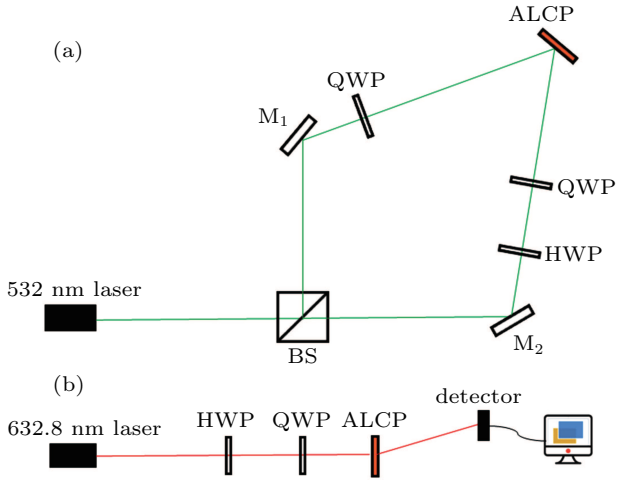


Fig. 4. The experimental optical paths of (a) recording the grating and (b) detecting the diffraction light of the grating. BS is a spectroscopic prism; M_1, M_2, and M_3 are reflective mirrors; QWP is a quarter-wave plate; HWP is a half-wave plate; and ALCP is the azo liquid crystal polymer film.

A 532 nm laser is used as the recording light. Firstly, the 532 nm laser is divided into two beams by using a spectroscopic prism. At this time, both beams have S-linear polarization. Then, one of the beams passes through a half-wave plate and becomes P-linearly polarized. Then, both beams pass through a quarter-wave plate; the S-linearly polarized light turns into right-handed circularly polarized light, and the P-linearly polarized light turns into left-handed circularly polarized light. Finally, two orthogonal circularly polarized light beams interfere on the azo liquid crystal film. The interference light field is recorded, and the orthogonal circular polarization grating is obtained.

In order to verify the function of the polarization grating as a beam deflector, a polarization state measure instrument was used to detect the polarization states of the detection light and diffraction light. The results are shown in Fig. 5.

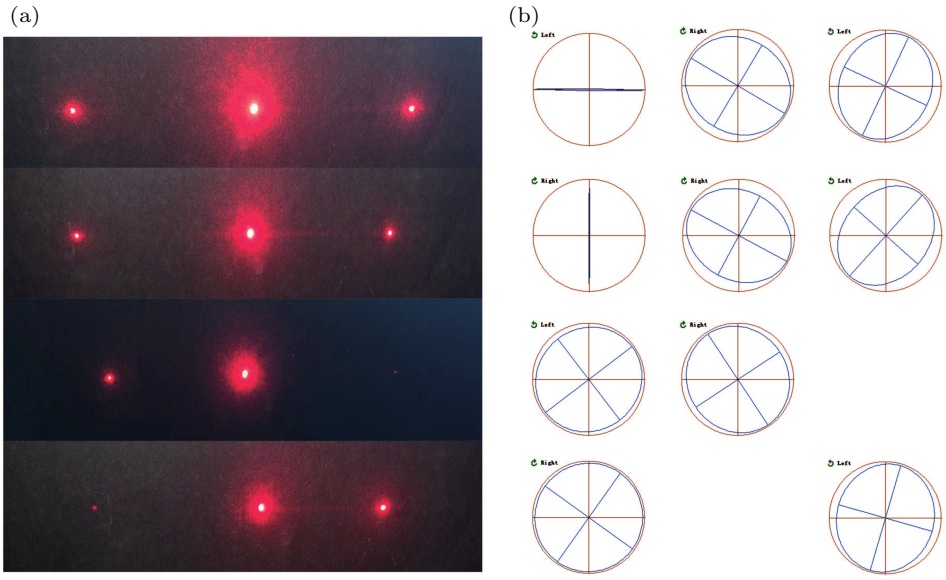


Fig. 5. (a) Diffraction patterns of polarization grating. (b) Polarization patterns of detection and diffraction light.

A 632.8 nm laser was used as as the detection light. From Fig. 5, we can see that when the detection light is P-linearly polarized, there are diffractions of -1 and $+1$ orders; moreover, the diffraction light of the -1 order is right-handed circularly polarized while the diffraction light of the $+1$ order is left-handed circularly polarized. When the detection light is S-linearly polarized, the diffraction mode is the same as that of the P-linearly polarized case. When the detection light is left-handed circularly polarized, the energy of the diffraction light is concentrated at the -1 order, and the -1 order diffraction light is left-handed circularly polarized. When the detection light is right-handed circularly polarized, the energy of the diffraction light concentrates at the order of $+1$, and the $+1$ diffraction light is left-handed circularly polarized. In the figure, it can be seen that when the detection lights of different polarizations incidents on the polarization grating, there is always a zeroth-order diffraction light. This is mainly because the thickness of the film does not exactly meet the half-wave condition of the wavelength. If this condition is satisfied, the zeroth-order diffraction light will disappear and the diffraction efficiency of the -1 or $+1$ order will reach 100% theoretically.

3.2. Coupling input structure of optical waveguide

The optical waveguide used in this design is a silicon-based optical wave. The structure of the system coupling input terminal is shown in Fig. 6.

In Fig. 6, the light incidents from the air layer of refractive index $n_0 = 1$, and is then diffracted by the azo liquid crystal polymer layer (refractive index $n_1 = 1.7$). The diffraction light refracts into the SiO_2 layer, whose refractive index is $n_2 = 1.5$. Finally, the light incidents on the interface of the SiO_2 and Si layers and refracts into the Si layer (refractive index $n_3 = 3.5$). To ensure total reflection of light in the silicon layer, the critical value of the angle θ is

$$\theta = \arcsin(n_2/n_3). \tag{1}$$

Therefore, the diffraction angle α of light passing through the polarization grating needs to satisfy

$$\alpha > \arcsin(n_2 \sin(\pi/2 - \varphi)/n_1), \tag{2}$$

where

$$\varphi = \arcsin(n_3 \sin(\pi/2 - \theta)/n_2). \tag{3}$$

Because the designed optical system needs to consider the different diffraction angles of light with different wavelengths incident on the polarization gratings, we studied the relationship between the diffraction angle and the incident angle. The experimental results are shown in Fig. 7.

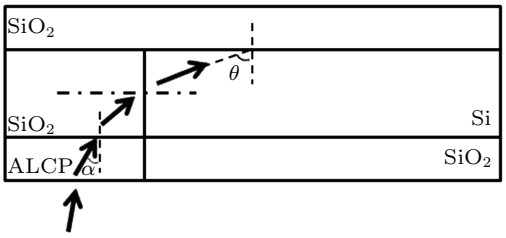


Fig. 6. Diagram of the coupling input structure of optical waveguide.

In Fig. 7, the red, green, and blue curves represent three incident lights of different wavelengths. It can be seen that the diffraction angle is linearly dependent on the incident angle. At the same incident angle, the diffraction angle of the red light with the longest wavelength is about 10° larger than that of the blue light with the shortest wavelength. The relationship between the diffraction angle and the wavelength can be expressed as

$$\Lambda \sin\theta = m\lambda_{\mathrm{d}}. \tag{4}$$

For a certain grating, the grating period Λ is fixed. We only study the -1 and $+1$ order diffractions of the polarization grating, and therefore $m = \pm 1$. The grating period can be changed by changing the angle between the two recording beams, and finally the diffraction angle is changed. The relationship between the grating period and the angle between the two recording beams can be expressed as

$$\Lambda = \lambda_{\mathrm{p}}/2\sin\beta, \tag{5}$$

where λ_{p} is the wavelength of the recording light and β is the angle between the two recording beams. Taking the 632.8 nm red light as an example, the relationship between the diffraction efficiency and the incident angle is studied in Fig. 8.

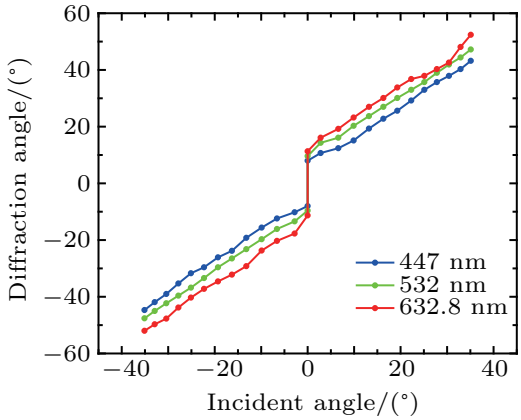


Fig. 7. Relationship between the incident angle and the diffraction angle.

Figure 8 shows a normalized curve of the diffraction efficiency of red light. When the incident angle is about $-6°$, the diffraction efficiency reaches the maximum. This is probably due to the recording optical path. When the incident angle changes from $-6°$ to $3°$, the diffraction efficiency decreases to 80% of the maximum value. Therefore, in practical application, the light should be incident at a small angle. When the incident angle changes from $-6°$ to $15°$, the diffraction efficiency decreases to 50% of the maximum value, and therefore the effective field of view of this system is about $30°$ in theory.

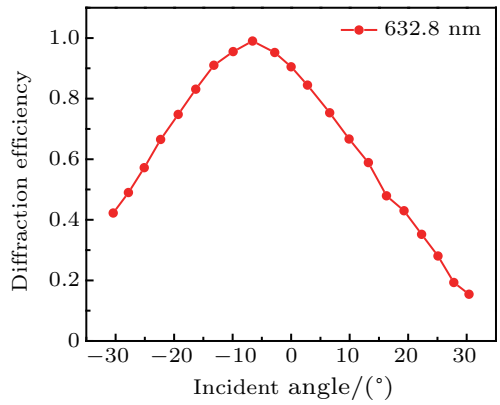


Fig. 8. Relationship between the incident angle and the diffraction efficiency.

4. Conclusion

A new optical system based on a polarization grating for AR display is proposed in this paper. The system utilizes the polarization selectivity of the polarization grating, and only one microprojector is needed to show different images to people's left and right eyes. At the same time, three polarization gratings are used at the coupling input structure of the optical waveguide. The efficiency of light coupling into the optical waveguide can be significantly improved by utilizing the single-order diffraction characteristics of the polarization grating. The thickness of the grating should meet the half-wave condition of the corresponding wavelength to realize high diffraction efficiency. In order to satisfy the total reflection condition $\theta = \arcsin(n_2/n_3)$, the diffraction angle of the polarization grating also needs to satisfy certain conditions:

$$\alpha > \arcsin\left(n_2 \sin\left(\pi/2 - \varphi\right)/n_1\right),$$

where $\varphi = \arcsin\left(n_3 \sin\left(\pi/2 - \theta\right)/n_2\right)$.

The polarization grating was recorded and its diffraction mode was studied. The relationship between the incident angle and the diffraction angle, and that between the incident angle and the diffraction efficiency, were also investigated to ensure the feasibility of this optical system in practice.

References

[1] Hu X D and Hua H 2015 *Appl. Opt.* **54** 9990
[2] Liu S X, Li Y, Zhou P C, Chen Q M, Li S D, Liu Y D, Wang Y F and Su Y K 2018 *J. Soc. Inf. Disp.* **26** 687
[3] Yoshida T, Tokuyama K, Takai Y, Tsukuda D, Kaneko T, Suzuki N, Anzai T, Yoshikaie A, Akutsu K and Machida A 2018 *SID Symp. Dig. Tech. Pap.* **49** 200
[4] Lee S, Jang C W, Moon S, Cho J and Lee B 2016 *ACM Trans. Graph.* **35** 60
[5] Maimone A, Lanman D, Rathinavel K, Keller K, Luebke D and Fuchs H 2014 *ACM Trans. Graph.* **33** 89
[6] Wu H K, Lee S W Y, Chang H Y and Liang J C 2013 *Comput. & Educ.* **62** 41
[7] Nicolau S, Soler L, Mutter D and Marescaux J 2011 *Surg. Oncol.* **20** 189
[8] Wang Y and Samaras D 2003 *Graph. Models* **65** 185
[9] Hong K, Yeom J, 1 Jang C W, Hong J and Lee B 2014 *Opt. Lett.* **39** 127
[10] Zhan T, Lee Y H and Wu S T 2018 *Opt. Express* **26** 4863
[11] Su Y F, Cai Z J, Liu Q, Shi L Y, Zhou F, Huang S S, Guo P L and Wu J H 2018 *Opt. Commun.* **428** 216
[12] Su Y F, Cai Z J, Liu Q, Guo P L, Lu Y F and Shi L Y 2017 *Optik* **149** 239
[13] Zheng Z R, Liu X, Li H F and Xu L 2010 *Appl. Opt.* **49** 3661
[14] Yun-Han L E E, Tao Z H A N and Shin-Tson W U 2019 *Virtual Reality & Intell. Hardware* **1** 10
[15] Chen H W, Weng Y S, Xu D M, Tabiryan V and Shin-Tson Wu 2016 *Opt. Express* **24** 7287
[16] Yu C, Peng Y F, Zhao Q, L I H and Liu X 2017 *Appl. Opt.* **56** 9390
[17] Wang Z, Dai P, Lv G Q and Feng Q B 2018 *IEEE Photon. J.* **10** 1109
[18] Liu Y Z, Pang X N, Jiang S J and Dong J W 2013 *Opt. Express* **21** 12068
[19] Liu S X, Li Y, Zhou P C, Chen Q M and Y K S U 2018 *Opt. Express* **26** 3394
[20] Liu S Q, Sun P, Wang C and Zheng Z R 2017 *Opt. Commun.* **403** 376
[21] Wang Q F, Cheng D W, Wang Y T, Hua H and Jin G F 2013 *Appl. Opt.* **52** C88

[22] Gao Q K, Liu J, Duan X H, Zhao T, Li X and Liu P L 2017 *Opt. Express* **25** 8412
[23] Kim S K, Kim E H and Kim D W 2011 *Opt. Eng.* **50** 114001
[24] Lee Y H, Tan G, Yin K, Zhan T and Wu S T 2018 *J. Soc. Inf. Disp.* **26** 64
[25] Zeng Y, Pan Z H, Zhao F L, Qin M, Zhou Y and Wang C S 2014 *Chin. Phys. B* **23** 024212
[26] Nikolova L and Todorov T 1984 *Opt. Acta* **31** 579
[27] Todorov T, Nikolov L and Tomova N 1984 *Appl. Optics* **23** 4588
[28] Todorov T, Nikolova L, Stoyanova K and Tomova N 1985 *Appl. Opt.* **24** 785
[29] Sutherl R L 2002 *J. Opt. Soc. Am. B* **19** 2995
[30] Crawford G P, Eakin J N, Radcliffe M D, Callan-Jones A and Pelcovits R A 2005 *J. Appl. Phys.* **98** 123102
[31] Nedelchev L, Ivanov D, Berberova N, Strijkova V and Nazarova D 2018 *Opt. Quantum Electron.* **50** 212
[32] Tabiryan V, Nersisyan R, Steeves M and Kimball R 2010 *Opt. Photon. News* **21** 40
[33] Lu W Q, Chen G Y, Hao Z F, Xu J J, Tian J G and Zhang C P 2010 *Chin. Phys. B* **19** 084208
[34] Abrahamyan V K 2015 *J. Contemp. Phys.* **50** 240
[35] Shishido A, Tsutsumi O, Kanazawa A, Shiono T, Ikeda T and Tamai N 1997 *J. Am. Chem. Soc.* **119** 7791
[36] Aristov A K, Novosel'skii V V, Semenov G B, Shchedrunova T V, Sohn H K and Yu M B 2003 *J. Opt. Technol.* **70** 480